CEA Comité Español de Automática
XLV JORNADAS AUTOMÁTICA MÁLAGA 2024
UNIVERSIDADE DA CORUÑA

Jornadas de Automática

Capturing Thermal Dynamics in Air-Conditioned Rooms: A Data-Driven Approach

Gómez-Ruiz, G.[a,*], Sánchez, A.J.[b], Sánchez-Herrera, R.[a], Andújar, J.M.[a]

[a] *Research Centre CITES, University of Huelva, 21007 Huelva, Spain.*
[b] *Department of Mechanical, Biomedical, and Manufacturing Engineering, Munster Technological University, Bishopstown, Cork, T12 P928, Ireland.*

To cite this article: Gómez-Ruiz, G., Sánchez, A.J., Sánchez-Herrera, R., Andújar, J.M. 2024. Capturing Thermal Dynamics in Air-Conditioned Rooms: A Data-Driven Approach. Jornadas de Automática, 45. https://doi.org/10.17979/ja-cea.2024.45.10818

Resumen

Las cargas termostáticamente controladas (TCL, por sus siglas en inglés de 'thermostatically controlled load') juegan un papel crucial en la reducción del consumo energético en los edificios. Por tanto, es esencial el desarrollo de modelos precisos que permitan una implementación efectiva de estrategias de control que reduzcan la demanda energética. Con este objetivo, se ha desarrollado un modelo que representa el comportamiento térmico de una habitación bajo la influencia de un aire acondicionado (AC), como punto de partida de nuestra investigación en el modelado y control de TCL. En concreto, se utilizó un enfoque de modelado basado en datos recogidos de una plataforma construida específicamente para este fin y un algoritmo diseñado para determinar los estados de operación del AC. Los resultados conseguidos, basados en las métricas del error cuadrático medio (RMSE, por sus siglas en inglés de 'root mean square error') y del error máximo absoluto (MAXAE, por sus siglas en inglés de 'maximum absolute error'), demostraron la efectividad del algoritmo propuesto y del modelo para capturar la dinámica térmica de la habitación bajo la influencia del AC.

Palabras clave: filtrado y suavizado, identificabilidad, identificación para control, software para identificación de sistemas, validación de modelos.

Capturing Thermal Dynamics in Air-Conditioned Rooms: A Data-Driven Approach

Abstract

Thermostatically controlled loads (TCLs) play a crucial role in reducing energy consumption in buildings. Thus, developing accurate models that enable the effective implementation of energy control strategies is essential. With this goal in mind, a model of a room influenced by an air conditioning (AC) unit was developed as an initial starting point for our research into TCL systems modeling and control. In this work, a data-driven modeling approach was utilized, employing data collected from an ad-hoc data collection platform. In addition, an algorithm was developed to determine the AC's operational states. The results, based on RMSE (Root Mean Square Error) and MAXAE (Maximum Absolute Error) metrics, demonstrate the effectiveness of the proposed algorithm and data-driven modeling approach in capturing the thermal dynamics of the room under the influence of the AC unit.

Keywords: filtering and smoothing, identifiability, identification for control, software for system identification, model validation.

1. Introduction

Thermostatically controlled loads (TCLs), particularly air conditioning (AC) systems, are significant energy consumers in buildings, accounting for approximately 40% of total energy usage ("International Energy Agency," 2023). This substantial consumption necessitates the implementation of effective energy conservation strategies in buildings. Various strategies have been explored and applied to achieve this goal, which can be grouped based on occupancy patterns and energy demand.

Strategies related to occupancy patterns include night setbacks and optimizing start and stop times. Night setbacks (Guo and Nutter, 2010) involve lowering heating set-points

*Autor para correspondencia: gabriel.gomez@diesia.uhu.es

or raising cooling set-points during nighttime hours when occupancy is minimal, thereby conserving energy. Optimizing start and stop times (Canbay, 2003) ensures that AC systems operate only when necessary, aligning closely with actual occupancy patterns and the thermal needs of the building.

On the other hand, strategies addressing energy demand include pre-cooling during off-peak periods and set-points changes during peak hours. Pre-cooling (Turner et al., 2015) takes advantages of lower energy costs by cooling the building during times when demand is low, reducing the need for cooling during peak hours. Adjusting set-point temperatures during peak hours (Braun and Kyoung-Ho Lee, 2006) helps to minimize energy use and cost when energy demand and prices are highest.

Based on the above, the implementation of advanced control strategies is essential. To this end, there are many approaches, such as Proportional-Integral-Derivative (PID) control (Soyguder et al., 2009), fuzzy logic control (Berouine et al., 2019), and neural network control (Li et al., 2013). It is worth mentioning that these methods do not require knowing the model of the system to implement the controller; however, an accurate model built beforehand can help in the controller design process.

In contrast, one of the most widely used control strategies in energy conservation, model predictive control (MPC) (Moroşan et al., 2010), requires a model to implement the control stage. This approach is highly effective and widely used in energy conservation due to its predictive and optimization capabilities (Berouine et al., 2022). Consequently, MPC will be the focus in our research into TCL modeling and control.

Therefore, developing a model that accurately reflects the system's behavior under a wide range of operating conditions is crucial. There are several modeling approaches to address this need: white-box, black-box, and gray-box models. White-box models (Beghi et al., 2011) are based on a deep understanding of the system physics and use manufacturer-supplied parameters to model system dynamics. These models, usually state space models, offer a good generalization capacity and are very suitable for control, however it is not always possible to obtain analytical expressions that faithfully reflect the dynamics of the system, so that simplifications (linearizations around set points, among others) are usually used, which limit both the accuracy of the model and its range of use. In contrast, black-box models, also called data-driven models (Afram and Janabi-Sharifi, 2015), are developed using experimental input-output data and fitting mathematical functions to these data. Although they can be very accurate, data-driven models often lack the physical meaning of the system under analysis. Gray-box models (Gomez-Ruiz et al., 2024; Liu et al., 2022) provide a balanced approach, combining the physical understanding of white-box models with the data-driven accuracy of black-box models. These models use the physics-based structure of white-box models and incorporate measured data to estimate model parameters, resulting in better accuracy and generalization capabilities compared to purely white-box or black-box approaches.

In this paper, the modeling of a room's thermal behavior influenced by a commercial AC unit using a data-driven modeling approach is presented. This approach was chosen with a view to designing a modeling methodology that would work well for systems whose analytical performance, based on equations reflecting their dynamics, is unknown. Additionally, it is considered the fastest way to develop the model since it relies solely on experimental data, which were collected using an ad-hoc (designed by the authors) data collection platform. However, a significant challenge emerged because the AC's operational states at each sampling interval were unknown due to inaccessibility of the machine's internal thermostat readings. To address this problem, an algorithm that detects the AC's operational states based on collected experimental data was developed.

Based on everything discussed above, the main contributions of this paper are the algorithm for detecting the AC's operational states and the development of the room's thermal behavior model.

The remainder of this paper is organized as follows: Section 2 presents an overview of the system under analysis, the proposed experimental setup, and the experimental data. Section 3 outlines the proposed algorithm for determining the AC's operational states. Section 4 details the room's thermal behavior modeling. Section 5 discusses the results and evaluates the performance of the models and the proposed algorithm. Finally, Section 6 summarizes the key contributions and suggests potential future work to enhance TCL system modeling and control.

2. Materials and methods

In this work, the thermal behavior of a room cooled by an AC unit within a controlled environment is studied. The experiment was conducted in a room with dimensions of 4 meters long, 3 meters wide and 3 meters high. The AC unit used is the Hisense® APC12Q model ("Air conditioning unit Hisense APC12QC," 2024), a commercially available unit designed for residential and small commercial applications with a power consumption of 1340W in refrigeration mode. Additionally, a data collection platform was developed to collect and analyze data during the experiment. This platform includes temperature sensors ("MCP9808," 2024) to measure both indoor and exterior room temperatures, a data acquisition board ("ESP32," 2024) and remote control switches ("SONOFF RFR2," 2024) to adjust the AC operating mode. All these elements communicate with MATLAB®, where the data is collected and analyzed. The experimental setup, comprising the room, the AC unit and the data collection platform with all elements involved, is shown in Figure 1.

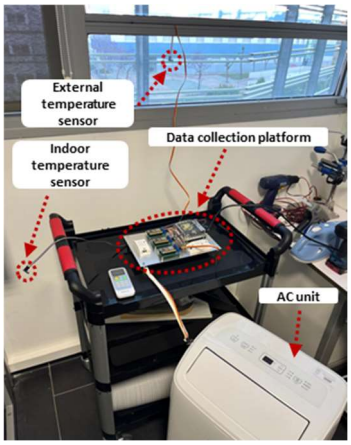

Figure 1: Experimental setup modeling the AC unit.

Using the proposed experimental setup, the AC unit was tested under various operating conditions, and both the indoor and exterior room temperature were measured. The experiment started at 10 am and finished at 4 pm, consisting of two consecutive refrigeration cycles. In each cycle, the AC initially operated in on mode for two hours, followed by a transition to off mode, which was maintained for one hour. Both exterior and indoor room temperatures were measured at intervals of 10 seconds. As depicted in Figure 2, the exterior temperature exhibited a progressive increase from morning until afternoon. Regarding the indoor temperature, the peaks observed around the indoor setpoint temperature, approximately 287K, indicate the influence of the AC thermostat. These peaks represent the operational state (ON or OFF) of the AC during its on mode.

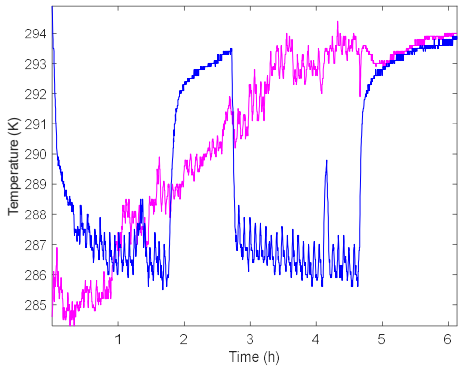

Figure 2: Indoor temperature (blue) and exterior temperature (magenta) measured during the experiment.

However, the sequence of the AC's operational states during the experiment is unknown because access to the thermostat readings was not possible, a limitation often encountered with commercial AC units. Therefore, to enable the proposed modeling approach, it is necessary to develop an algorithm capable of determining the sequence of the AC's operational states.

3. AC Operational State Detection Algorithm (AC-OSDA)

In this section, the algorithm capable of detecting the AC's operational states (AC-OSDA) is introduced. Employing a systematic approach, the AC-OSDA is represented by a comprehensive flowchart outlining the sequential steps of the proposed algorithm, as illustrated in Figure 3. This flowchart guides the determination of the AC's operational states based on the indoor temperature data presented in Figure 2.

The algorithm begins by collecting the indoor room temperature data denoted as T_{ie} and then filters it using (1).

$$T_{ief}(k) = \frac{1}{N}\sum_{i=0}^{N-1} T_{ie}(k-i) \quad (1)$$

Where T_{ief} represents the filtered indoor room temperature at each sampling interval k. Here, k is an element of the set {1, 2, …, N}, with N being the total number of samples in the experiment.

Subsequently, the algorithm calculates the difference between the current and the previous values of T_{ief} as indicated in (2):

$$\Delta T_{ief}(k) = T_{ief}(k+1) - T_{ief}(k) \quad (2)$$

By observing values of ΔT_{ief} close to zero, the algorithm identifies peaks in the indoor temperature signal. To accomplish this, the algorithm evaluates if the value of ΔT_{ief} falls within the range $-\Delta_o < \Delta T_{ief}(n) < \Delta_o$, where Δ_o represents the limit value of ΔT_{ief} around zero used for identifying peaks in the signal.

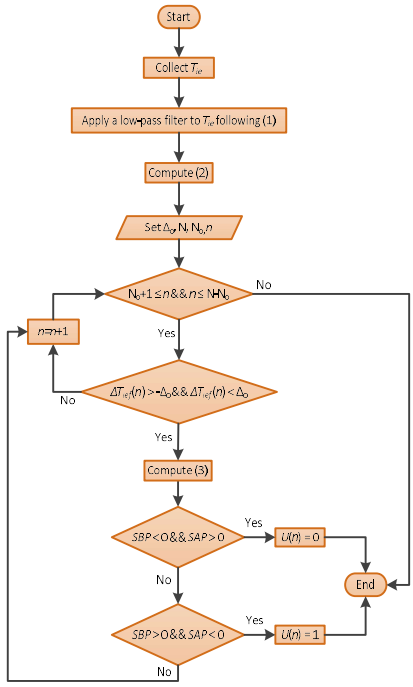

Figure 3: Flowchart illustrating the steps of AC-OSDA.

Upon identifying a peak, the algorithm determines the sum of ΔT_{ief} taken for N_o values before and after the peak, following (3):

$$SBP = \sum_{i=1}^{N_o} \Delta T_{ief}(n-i)$$
$$SAP = \sum_{i=1}^{N_o} \Delta T_{ief}(n+i) \quad (3)$$

Where SBP represents the sum of ΔT_{ief} values before the peak, and SAP represents the sum of ΔT_{ief} values after the peak. Here, n is an element of the set $\{N_o+1, N_o+2, \ldots, N-N_o\}$.

Based on the values of SBP and SAP, the algorithm discerns whether the peak corresponds to a local minimum or maximum. For instance, if the value of the sum before the peak is negative and after the peak is positive, it indicates a local minimum. In this case, the AC's operational state is set to 0. Conversely, for a local maximum, the AC's operational state is set to 1. Finally, the algorithm concludes its execution.

The performance of applying AC-OSDA to indoor room temperature data mainly depends on the values of Δ_o and N_o, as shown in Figure 3. A procedure for assessing the algorithm's performance was proposed.

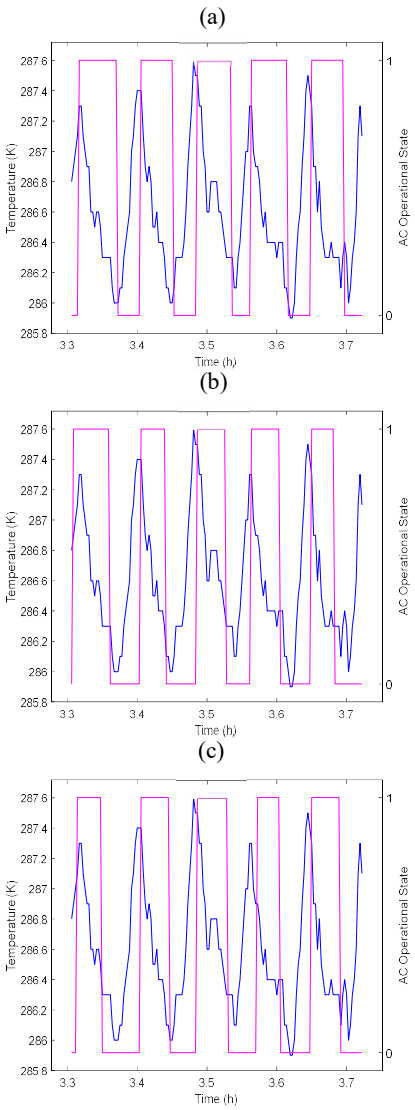

Figure 4: Comparison between the indoor temperature without filtering (blue) and the AC's operational states provided by AC-OSDA (magenta), considering the following parameter settings: (a) $N_o = 6$ and $\Delta_o = \pm 0.05$, (b) $N_o = 12$ and $\Delta_o = \pm 0.05$, and (c) $N_o = 18$ and $\Delta_o = \pm 0.05$.

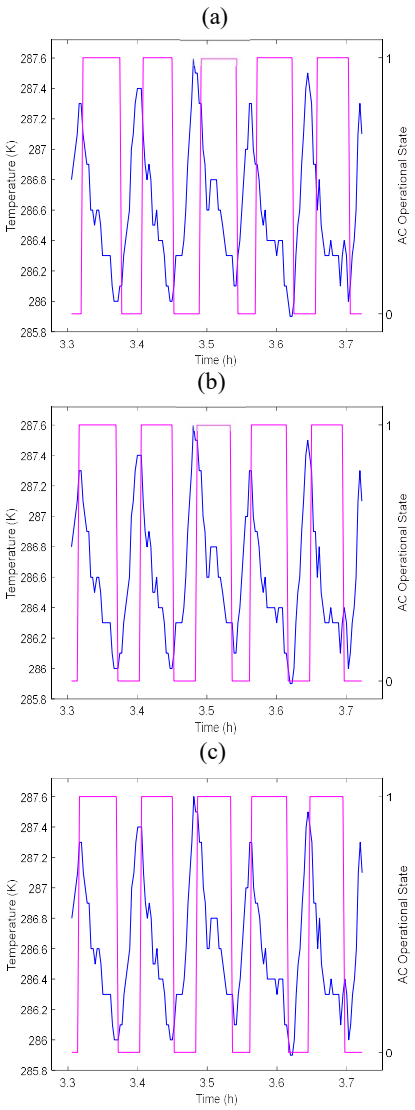

Figure 5: Comparison between the indoor temperature without filtering (blue) and the AC's operational states provided by AC-OSDA (magenta), considering the following parameter settings: (a) $N_o = 6$ and $\Delta_o = \pm 0.01$, (b) $N_o = 6$ and $\Delta_o = \pm 0.05$, and (c) $N_o = 6$ and $\Delta_o = \pm 0.1$.

First, one of the parameters was fixed, and different values were set for the other. Next, the same procedure was applied in reverse. The values for the parameters were logically set after observing experimental data. For Δ_o, the values were selected based on the mean values of ΔT_{ief} around zero when a peak is observed. For N_o, the values were chosen to represent the values of ΔT_{ief} one minute, two minutes, and three minutes before and after the peak. The results of these simulations are presented in Figure 4 and 5.

In the first three cases, the value of Δ_o was set to ±0.05, while the value of N_o was set to 6, 12, and 18, as can be seen in Figure 4(a), Figure 4(b), and Figure 4(c), respectively. It is evident that increasing the value of N_o does not improve the detection of the peaks, particularly the detection of the minimum peaks. Based on the main conclusion drawn from the results shown in Figure 4, in the next three simulations the value of N_o was set to 6, and the value of Δ_o was initially set to ±0.01, then adjusted to ±0.05, and finally to ±0.1, as can be seen in Figure 5(a), Figure 5(b), and Figure 5(c), respectively. It can be observed that the performance in Figure 5(a) shows a delay in the detection of the operational states, while in Figures 5(b) and 5(c), the delay is minimum.

The results provided in Figure 5(c) are considered the best since the range of evaluation is wider than in the results shown in Figure 5(b) with approximately the same performance. Therefore, in the proposed study, the values of Δ_o and N_o were chosen according to a logical interpretation of the results shown in Figures 4 and 5. Based on this, the parameter setting with $N_o = 6$ and $\Delta_o = \pm 0.1$ was used for the data-driven modeling approach presented in the next section.

4. Data-driven modeling

In this section, a data-driven modeling approach is employed to accurately capture the temperature dynamics within the room influenced by the AC unit. Specifically, two distinct mathematical models were identified based on experimental data: a state-space (SS) model and an AutoRegressive with eXogenous inputs (ARX) model. These models were chosen because they provided excellent results in the ranking established by (Afram and Janabi-Sharifi, 2015) after developing different types of models using experimental data. The input and output variables considered in the modeling process are: the external temperature, gathered by the data collection platform outlined in Section

2, and the AC's operational states, determined by the algorithm presented in Section 3, as inputs; and the indoor temperature as output, thus configuring a multiple-input, single-output (MISO) model. Both model representations, i.e., the SS and ARX models, were identified using MATLAB®. Model order selection followed the guidelines provided in (Afram and Janabi-Sharifi, 2015), aiming to keep the model order low unless increasing it provided significant benefits. To address the issue of overfitting, 80% of the dataset was allocated for modeling, while the remaining 20% was reserved for validation.

4.1. SS identified model

The SS identified model describes the room's thermal behavior in terms of its states, inputs and outputs. The SS identified model equations are given by (4):

$$\begin{aligned} x(k+1) &= \mathrm{A}\cdot x(k)+\mathrm{B}\cdot u(k)+\mathrm{K}\cdot e(k) \\ y(k) &= \mathrm{C}\cdot x(k)+\mathrm{D}\cdot u(k)+e(k) \end{aligned} \tag{4}$$

Where, for each sampling time k, $x(k)$ represents the state vector, composed of the variables in the energy storage elements in the room; $u(k)$ represents the input vector, composed of the external temperature and the AC's operational states; $y(k)$ represents the output vector; $e(k)$ represents the disturbance vector, taking into account system inaccuracies, variations in matrix values and external disturbances.

The algorithm used in MATLAB ("n4sid," 2024), provided state-space matrices A, B, C, D, and K, along with their involved coefficients. The SS matrices of the identified model are given as follows (5) - (9):

$$\mathrm{A}=\begin{bmatrix} 0.9769 & -0.0328 \\ -0.0337 & 0.8202 \end{bmatrix} \tag{5}$$

$$\mathrm{B}=\begin{bmatrix} 4.7447\cdot 10^{-4} & -0.0022 \\ 0.0028 & -6.7910\cdot 10^{-4} \end{bmatrix} \tag{6}$$

$$\mathrm{C}=\begin{bmatrix} 84.4214 & 0.3713 \end{bmatrix} \tag{7}$$

$$\mathrm{D}=\begin{bmatrix} 0 & 0 \end{bmatrix} \tag{8}$$

$$\mathrm{K}=\begin{bmatrix} 0.008623 \\ -0.002862 \end{bmatrix} \tag{9}$$

By analyzing the state matrix, A, it was concluded that the proposed SS identified model for the room's thermal behavior is a second-order model, involving two states variables that may represent the indoor temperature and the wall room temperature. It is worth nothing that the experimental data involved only the indoor temperature to represent the system's dynamics, while this model involves two variables. This allows for a better characterization of the system.

4.2. ARX model

The ARX model captures the room's thermal behavior using input-output data. The ARX model equation, with the involved polynomials $A(z)$, $B_1(z)$, and $B_2(z)$, is expressed in (10):

$$y(k) = A(z)\cdot y(k) + B_1(z)\cdot u_1(k) + B_2(z)\cdot u_2(k) \tag{10}$$

Where, for each sampling time k, $y(k)$ denotes the output while $u_1(k)$ and $u_2(k)$ represent the input variables. These inputs are the same as in the SS identified model.

The polynomials of the ARX model for the output $y(k)$ were identified using ("arx," 2024), and they are given as follows (11) - (13):

$$A(z) = 1-0.9721z^{-1}-0.1143z^{-2}+0.09674z^{-3}+0.007063z^{-4} \tag{11}$$

$$B_1(z)=0.02555+0.01548z^{-1}+0.007359z^{-2}-0.05075z^{-3} \tag{12}$$

$$B_2(z)=-0.09051-0.03316z^{-1}-0.03325z^{-2}-0.0237z^{-3} \tag{13}$$

In that case, the order of the system is determined by observing the highest order of the polynomials in the model, therefore it is concluded that the ARX model is of fourth-order.

5. Results and Discussion

In this section, the simulated responses of the room's thermal behavior model using both representations, i.e., the SS model and ARX model, are presented. Additionally, the visual comparison with the measured response is provided and analyzed. To evaluate the accuracy of the model in both representations, two analytical metrics were used: RMSE (Root Mean Square Error) and MAXAE (Maximum Absolute Error).

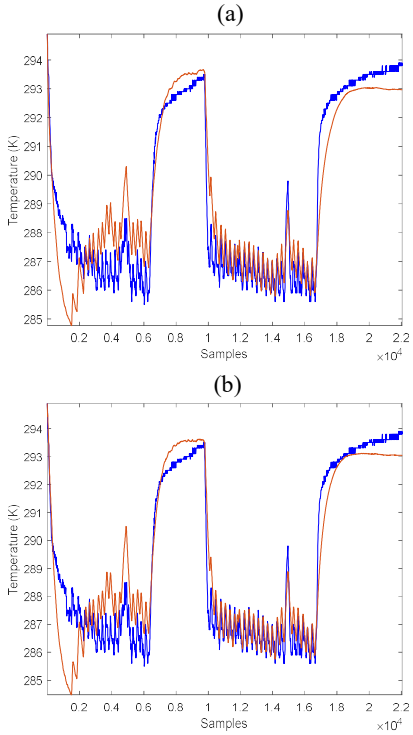

Figure 6: Measured (blue) and simulated (orange) responses of room's thermal behavior model: (a) SS identified model, and (b) ARX model.

As depicted in Figure 6, both models demonstrated a reasonable level of accuracy in predicting the indoor room temperature. This also indicates that the AC's operational states provided by AC-OSDA were appropriate. However, common challenges were observed in both models, such as accurately capturing the dynamics during the initial

refrigeration cycle and predicting the settling behavior when the AC transitions to the off mode. This may because there are fewer data points in these regions compared to the regions where the thermostat frequently changes the operational state of the AC. According to the analytical metrics presented in Table 1, both models are evaluated based on their RMSE and MAXAE values, expressed in K.

Table 1: RMSE and MAXAE for the simulation of the SS and ARX models.

Accuracy index	Model	In this work	(Afram and Janabi-Sharifi, 2015)
RMSE	SS	1.0489K	0.716K
	ARX	1.0020K	0.777K
MAXAE	SS	3.1842K	3.438K
	ARX	3.4753K	4.273K

It is worth noting that lower values indicate better performance for both metrics. The RMSE value for the ARX model is lower compared to the SS identified model, suggesting that the ARX model performs slightly better in terms of overall accuracy. While the MAXAE value is higher for the ARX model, it is essential to consider that MAXAE represents a single point of error, a challenge observed in both models. Additionally, the RMSE and MAXAE values obtained in this work are consistent with those reported in similar studies (Afram and Janabi-Sharifi, 2015), as shown in Table 1.

6. Conclusion

In this work, the thermal behavior model of a room influenced by an AC unit was identified and represented using both SS and ARX models. The AC's operational states (unknown a priori) were effectively predicted using the proposed AC-OSDA. Evaluation of model performance, employing RMSE and MAXAE metrics, indicates that both identified models achieved a satisfactory level of accuracy, with the ARX model demonstrating slightly higher precision compared to the SS identified model. These findings, consisting with existing literature, validate the efficacy of the models and the employed algorithm.

The methodology used in this work represents the starting point for our research in TCL modeling and control, with potential for further improved. This includes testing the proposed algorithm with new datasets involving more data points. Future work should prioritize improving the interpretability of the model and establishing a procedure applicable to a broader range of TCL systems. To this end, the authors are currently developing a novel system modeling procedure that incorporates a gray-box modeling approach, suitable for various TCL systems. Of course, the ultimate goal of the research is to have the best possible model to apply model-based control techniques.

Acknowledgements

This research was conducted as part of the grant PID2020-117828RB-I00 funded by MICIU / AEI / 10.13039 / 501100011033 and, by Spanish Ministry of Science, Innovation and Universities. Furthermore, the corresponding author is supported by an FPU grant from the Spanish Ministry of Universities for training university teaching staff during their PhD period.

References

Afram, A., Janabi-Sharifi, F., 2015. Black-box modeling of residential HVAC system and comparison of gray-box and black-box modeling methods. Energy Build. 94, 121–149. https://doi.org/10.1016/j.enbuild.2015.02.045

Air conditioning unit Hisense APC12QC, 2024. URL https://www.hisense.es/aire-acondicionado-domestico/portatil/aire-acondicionado-portatil-apc12qc/ (accessed 5.14.24).

arx, 2024. URL https://es.mathworks.com/help/ident/ref/arx.html (accessed 5.28.24).

Beghi, A., Cecchinato, L., Paggiaro, F., Rampazzo, M., 2011. VAVAC systems modeling and simulation for FDD applications. Presented at the 2011 9th IEEE International Conference on Control and Automation (ICCA), IEEE, Santiago, Chile, pp. 800–805. https://doi.org/10.1109/ICCA.2011.6138039

Berouine, A., Akssas, E., Naitmalek, Y., Lachhab, F., Bakhouya, M., Ouladsine, R., Essaaidi, M., 2019. A Fuzzy Logic-Based Approach for HVAC Systems Control. Presented at the 2019 6th International Conference on Control, Decision and Information Technologies (CoDIT), IEEE, Paris, France, pp. 1510–1515. https://doi.org/10.1109/CoDIT.2019.8820356

Berouine, A., Ouladsine, R., Bakhouya, M., Essaaidi, M., 2022. A predictive control approach for thermal energy management in buildings. Energy Rep. 8, 9127–9141. https://doi.org/10.1016/j.egyr.2022.07.037

Braun, J.E., Kyoung-Ho Lee, 2006. An Experimental Evaluation of Demand Limiting Using Building Thermal Mass in a Small Commercial Building. ASHRAE Trans. 112, 559–571.

Canbay, Ç.S., 2003. Optimization of Hvac Control Strategies by Building Management Systems Case Study: Özdilek Shopping Center (M.Sc.). Ann Arbor, United States.

ESP32, 2024. URL https://www.espressif.com/en/products/socs/esp32 (accessed 5.27.24).

Gomez-Ruiz, G., Sanchez-Herrera, R., Andujar, J.M., Rubio Sanchez, J.L., 2024. Simulation-Based Education Tool for Understanding Thermostatically Controlled Loads. Sustainability 16, 999. https://doi.org/10.3390/su16030999

Guo, W., Nutter, D.W., 2010. Setback and setup temperature analysis for a classic double-corridor classroom building. Energy Build. 42, 189–197. https://doi.org/10.1016/j.enbuild.2009.08.014

International Energy Agency, 2023. URL https://www.iea.org/energy-system/buildings/space-cooling (accessed 5.17.24).

Li, S., Ren, S., Wang, X., 2013. HVAC room temperature prediction control based on neural network model. Presented at the 5th International Conference on Measuring Technology and Mechatronics Automation (ICMTMA), IEEE, New York, pp. 606–609. https://doi.org/10.1109/ICMTMA.2013.151

Liu, M., Tian, Y., Cheng, D., Zhang, Y., Ding, L., 2022. Modelling and control of central air-conditioning loads for power system emergency frequency control. IET Gener. Transm. Distrib. 16, 4054–4067. https://doi.org/10.1049/gtd2.12571

MCP9808, 2024. URL https://www.microchip.com/en-us/product/mcp9808 (accessed 5.24.24).

Moroşan, P.-D., Bourdais, R., Dumur, D., Buisson, J., 2010. Building temperature regulation using a distributed model predictive control. Energy Build. 42, 1445–1452. https://doi.org/10.1016/j.enbuild.2010.03.014

n4sid, 2024. URL https://es.mathworks.com/help/ident/ref/n4sid.html#mw_a7743737-84cd-49b8-bf91-971f4c0246f8 (accessed 5.27.24).

SONOFF RFR2, 2024. URL https://sonoff.tech/product/diy-smart-switches/rfr2/ (accessed 5.24.24).

Soyguder, S., Karakose, M., Alli, H., 2009. Design and simulation of self-tuning PID-type fuzzy adaptive control for an expert HVAC system. Expert Syst. Appl. 36, 4566–4573. https://doi.org/10.1016/j.eswa.2008.05.031

Turner, W.J.N., Walker, I.S., Roux, J., 2015. Peak load reductions: Electric load shifting with mechanical pre-cooling of residential buildings with low thermal mass. Energy 82, 1057–1067. https://doi.org/10.1016/j.energy.2015.02.011